

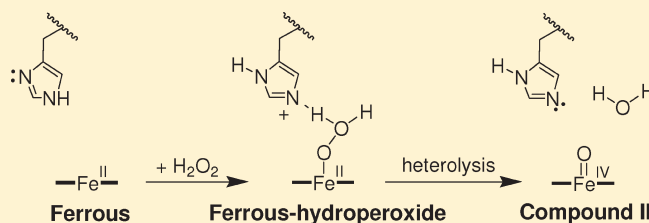
Reactivity of Deoxy- and Oxyferrous Dehaloperoxidase B from *Amphitrite ornata*: Identification of Compound II and Its Ferrous–Hydroperoxide Precursor

Jennifer D'Antonio and Reza A. Ghiladi*

Department of Chemistry, North Carolina State University, Raleigh, North Carolina 27695-8204, United States

Supporting Information

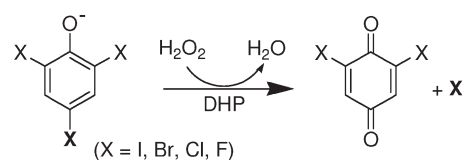
ABSTRACT: Dehaloperoxidase (DHP) from the terebellid polychaete *Amphitrite ornata* is a bifunctional enzyme that possesses both hemoglobin and peroxidase activities. The bifunctional nature of DHP as a globin peroxidase appears to be at odds with the traditional starting oxidation state for each individual activity. Namely, reversible oxygen binding is only mediated via a ferrous heme in globins, and peroxidase activity is initiated from ferric centers and to the exclusion of the oxyferrous oxidation state from the peroxidase cycle. Thus, to address what appears to be a paradox, herein we report the details of our investigations into the DHP catalytic cycle when initiated from the deoxy- and oxyferrous states using biochemical assays, stopped-flow UV–visible, and rapid-freeze-quench electron paramagnetic resonance spectroscopies, and anaerobic methods. We demonstrate the formation of Compound II directly from deoxyferrous DHP upon its reaction with hydrogen peroxide and show that this occurs both in the presence and in the absence of trihalophenol. Prior to the formation of Compound II, we have identified a new species that we have preliminarily attributed to a ferrous–hydroperoxide precursor that undergoes heterolysis to generate the aforementioned ferryl intermediate. Taken together, the results demonstrate that the oxyferrous state in DHP is a peroxidase competent starting species, and an updated catalytic cycle for DHP is proposed in which the ferric oxidation state is not an obligatory starting point for the peroxidase catalytic cycle of dehaloperoxidase. The data presented herein provide a link between the peroxidase and oxygen transport activities, which furthers our understanding of how this bifunctional enzyme is able to unite its two inherent functions in one system.



A number of sediment-dwelling marine polychaetes and hemichordates employ haloperoxidases to produce high levels of volatile brominated secondary metabolites as defense mechanisms.^{1,2} *Notomastus lobatus* (polychaeta)^{3–5} and *Saccoglossus kowalevskii* (hemichordata)^{6,7} are but two examples of marine worms that contaminate benthic ecosystems by secreting a diverse array of toxic haloaromatic compounds such as mono-, di-, and tribromophenols, mono- and dibromovinylphenols, and bromopyrroles. Thus, either by exposure to these toxins through contact upon burrowing or via ingestion by deposit feeders, environmental sediments that are contaminated with these biogenically produced halometabolites represent a significant challenge to other infaunal organisms that co-inhabit coastal mudflats. One such organism, the terebellid polychaete *Amphitrite ornata*, has been shown to be tolerant to bromometabolite toxicity because of the production of dehalogenating enzymes, and in particular dehaloperoxidase (DHP). Evidence suggests that this bifunctional protein serves as both an intracellular, monomeric coelomic hemoglobin and a peroxidase that confers haloaromatic toxin resistance via oxidation of mono-, di-, and trisubstituted halophenols that possess bromine, chlorine, or fluorine substituents.^{8,9} Thus, as the first hemoglobin identified to possess a biologically relevant peroxidase activity,⁸ and as an example of globins found in marine organisms, structural and mechanistic

investigations of dehaloperoxidase may reveal new insights into the structure–function paradigms of the globin superfamily specific to bi- and multifunctional proteins.

Several recent studies have focused on elucidating the structural, spectroscopic, and mechanistic details of ferric DHP.^{9–24} *A. ornata* possesses two separate genes (*dhpA* and *dhpB*) that encode a pair of DHP isoenzymes, termed DHP A and DHP B,²⁵ and both have been shown to catalyze the oxidative degradation of 2,4,6-trihalogenated phenols to the corresponding 2,6-dihalo-1,4-benzoquinones in the presence of hydrogen peroxide.



A combination of stopped-flow UV–visible and rapid-freeze-quench electron paramagnetic (EPR) spectroscopic methods has provided strong evidence that ferric DHP reacts with hydrogen

Received: March 1, 2011

Revised: May 29, 2011

Published: May 29, 2011

peroxide to yield Compound ES, an iron(IV)–oxo heme center with an amino acid radical.¹⁰ The catalytic competency of that intermediate in oxidizing trihalophenol cosubstrates 2,4,6-trichlorophenol (TCP) to dichloroquinone (DCQ) via a peroxidase-like catalytic cycle for DHP has been demonstrated, and evidence suggests that the overall two-electron oxidation of TCP by DHP proceeds through discrete one-electron steps.²¹ Interestingly, DCQ itself is not an innocent species, having been shown to react separately with both Compound ES and ferric DHP to yield oxyferrous DHP in either case.²⁶ As deduced by spectroelectrochemistry, the unusually high reduction potential for a peroxidase of 206 mV reported for DHP B likely facilitates reactions with DCQ that ultimately favor the reduction of the heme prosthetic group and formation of oxyferrous DHP B.²⁶ Thus, dichloroquinone chemistry may represent one possible link between the two activities of the bifunctional dehaloperoxidase by permitting the ferric state either to initiate a peroxidase pathway in the presence of TCP and H₂O₂ or to form the oxyferrous complex in the presence of DCQ (itself generated from the aforementioned peroxidase pathway), thus allowing O₂ transport function.

While progress has been made toward understanding the DCQ-driven functional switch in how the peroxidase-active ferric DHP state can be converted to the oxygen-binding ferrous form, our understanding of the reverse, wherein oxyferrous DHP is activated toward peroxidase function, is still lacking. Given that reversible oxygen binding is mediated via only a ferrous heme in globins and that peroxidase activity is initiated from ferric centers and to the exclusion of the oxyferrous oxidation state from the peroxidase cycle,²⁷ the bifunctional nature of DHP as a globin peroxidase paradoxically appears to be at odds with the traditional starting oxidation state for each individual activity. Recently, however, in a peroxidase reaction that is unique to DHP, both we²⁶ and Dawson and co-workers²⁸ have reported that dehaloperoxidase activity has been observed when the catalytic cycle is initiated from the oxyferrous state, but that the catalytically active species is formed only in the presence of the TCP cosubstrate. This observation suggests that substrate binding is the key to the functional switch of DHP from an oxygen-binding protein to a peroxidase. Thus, understanding how the substrate interacts with DHP to bring about this functional switch is a critical question that can significantly advance our comprehension of the dehaloperoxidase mechanism.

Using data derived primarily from stopped-flow UV–visible spectroscopic methods, one possibility that has been posited by Dawson and co-workers is that oxyferrous DHP is activated by TCP• radicals, themselves formed from trace amounts of the ferric enzyme reacting with TCP and hydrogen peroxide. The TCP• radicals thus generated oxidize the oxyferrous enzyme, generating bulk ferric DHP that is then responsible for the observed dehaloperoxidase activity. This supposition has precedent with the monofunctional lignin peroxidase (LiP), where veratryl alcohol oxidation has been shown to yield radical species that oxidize oxy-LiP to the peroxidase-active form. It has also been postulated by Franzen and co-workers that both external and internal small-molecule binding sites may exist with regulatory implications for the distal histidine, His⁵⁵, that may govern how DHP switches between its hemoglobin and peroxidase activities.^{11–13} It has been suggested that His⁵⁵, which has been observed in distinct “open” and “closed” conformations, mediates the displacement of O₂ from the heme in the presence of (tri)halophenol substrate, possibly serving as a trigger for peroxidase

function.¹¹ Typically, the Fe–His N^{ε2} distances in globins range between 4.1–4.6 and 5.5–6.0 Å for peroxidases.^{29–32} By comparison, in dehaloperoxidase, the Fe–His N^{ε2} distance is 5.5 Å³³ in ferric DHP B and between 4.8 and 5.5 Å in DHP A,^{17,34,35} when the distal histidine is in the closed position, and is 5.1 Å in oxyferrous DHP A. With His⁵⁵–O(1) (iron-bound) and His⁵⁵–O(2) (terminal) distances of 3.2 and 2.8 Å,¹⁷ respectively, oxyferrous DHP exhibits similarities to wild-type Mb in that the distal histidine interacts with both of the oxygen atoms of the end-on bound dioxygen ligand, while at the same time ferric DHP has a longer Fe–His N^{ε2} distance that more resembles those of peroxidases. Thus, the distal histidine–heme distance in dehaloperoxidase, being intermediate between those found in globins and peroxidases, is well positioned to function as both a stabilizer of the bound dioxygen ligand in the former and the general acid/base that facilitates both the deprotonation and heterolytic O–O bond cleavage of hydrogen peroxide in the latter.

Although counter to conventional peroxidase thinking, one possibility, based upon the premise that a common starting point is the most efficient pathway for a bifunctional enzyme to perform its dual roles, may be that peroxidase active intermediates are formed directly from the oxyferrous/ferrous state(s) in DHP, thereby permitting a peroxidase catalytic cycle to be initiated from the oxyferrous, and not ferric, state. Thus, the focus of this report is to provide insight into how trihalophenol binding activates both deoxyferrous and oxy-DHP toward peroxidase activity. As such, we present anaerobic UV–visible spectroscopic and kinetic studies of the reaction of deoxyferrous DHP B with hydrogen peroxide and provide evidence of the direct formation of the peroxidase-active Compound II intermediate that is formed in the absence of the trihalophenol cosubstrate. Evidence of a transiently formed ferrous–hydroperoxide species as a precursor to Compound II will be provided. Additionally, stopped-flow UV–visible and rapid-freeze-quench EPR spectroscopic studies of the reaction of oxyferrous DHP with H₂O₂ and trihalophenol, under conditions that have yet to be reported, will also be presented, thereby providing the basis for an alternative mechanism for the activation of oxyferrous DHP. Taken together, our experimental design reveals new mechanistic insights and kinetic descriptions of the dehaloperoxidase mechanism, which when interpreted in light of a mechanistic role for the conformational flexibility of the distal histidine (His⁵⁵)³³ advances our understanding of how DHP performs its dual functions and resolves the dehaloperoxidase paradox.

■ MATERIALS AND METHODS

Materials. Buffer salts were purchased from Fisher Scientific. All other reagents and biochemicals, unless otherwise specified, were of the highest grade available from Sigma-Aldrich. Solutions of trihalogenated phenols were freshly prepared prior to each experiment in 100 mM potassium phosphate (KP_i) buffer (variable pH), kept at 4 °C, and protected against light. UV–visible spectra were recorded periodically to ensure that the cosubstrate had not degraded by monitoring its absorbance: trifluorophenol, 270 nm (1027 M⁻¹ cm⁻¹);²⁶ trichlorophenol, 312 nm (3752 M⁻¹ cm⁻¹);¹⁰ tribromophenol, 316 nm (5055 M⁻¹ cm⁻¹).²⁶ Hydrogen peroxide solutions were also freshly made prior to each experiment. Initially, a 10 mM stock solution of H₂O₂ was prepared and maintained on ice (typically less than 15 min), during which all other protein/substrate solutions were loaded

into the stopped-flow apparatus or utilized for kinetic assays. When prepared in this manner, the stock H_2O_2 solution did not exhibit any degradation over this time period as determined by UV–visible spectroscopic analysis of the hydrogen peroxide absorbance at 240 nm ($\epsilon_{240} = 43.6 \text{ M}^{-1} \text{ cm}^{-1}$).³⁶ For stopped-flow and freeze-quench experiments, the stock H_2O_2 solution was then diluted to the appropriate premixing concentration and immediately loaded into the stopped-flow apparatus. Wild-type (WT) DHP isoenzyme A and B (six-His-tagged protein) expression and purification procedures were performed as previously described,^{10,12} and only protein samples that exhibited Reinheitszahl values (R_z) greater than 4.0 were utilized in this study. Optical spectra were recorded on either an Agilent 8453 diode array spectrophotometer or a Cary 50 UV–visible spectrophotometer, each equipped with thermostated cell holders at 25 °C. ³¹P NMR spectra were recorded on a Bruker 300 MHz NMR spectrometer, and chemical shifts are reported as δ values referenced to an external standard of trimethyl phosphate ($\delta = 0$ ppm). Ferrous DHP B samples for spectroscopic characterization were prepared in an MBraun LabMaster 130 inert atmosphere (<1 ppm O_2 , <1 ppm H_2O) glovebox under a nitrogen atmosphere. The spin trap DIPPMO was synthesized and characterized according to published procedures.³⁷

Preparation of Oxyferrous DHP B. Oxyferrous DHP B was generated via incubation of the ferric enzyme with 5 equiv of ascorbic acid in 100 mM KP_i (variable pH). Excess reducing agent was removed by using a PD-10 desalting column prepacked with Sephadex G-25 medium. The protein was concentrated using an Amicon Ultra centrifugal device equipped with a 10 kDa molecular mass cutoff membrane. Protein concentrations were determined using a heme molar absorption coefficient of $117.6 \text{ mM}^{-1} \text{ cm}^{-1}$ ($\lambda_{\text{max}} = 407 \text{ nm}$) for both the ferric²⁶ and oxyferrous states of the enzyme. The formation of the oxyferrous species was monitored by its UV–visible spectrum [418 (Soret), 542, and 578 nm].^{10,26}

Preparation of Ferrous DHP B. Ferrous DHP B was prepared by purging a ferric DHP B solution (100 mM KP_i , variable pH) for at least 20 min with argon. Then, the degassed enzyme solution was placed inside the glovebox and titrated with substoichiometric aliquots of sodium dithionite, itself dissolved in anaerobic buffer. Formation of ferrous DHP B was followed by UV–visible spectroscopy using an all quartz immersion probe (Hellma) that was connected to the spectrometer located outside of the glovebox via a fiber optic cable.

Stopped-Flow UV–Visible Spectrophotometric Studies. Experiments were performed on a Bio-Logic SFM-400 triple-mixing stopped-flow instrument equipped with a diode array UV–visible spectrophotometer and were conducted at 20 °C in 100 mM KP_i buffer (variable pH). A constant temperature of 20 °C was maintained using a circulating water bath. Data were collected (900 scans total) over a three-time domain regime (2.5, 25, and 250 ms; 300 scans each) using Bio Kinet32 (Bio-Logic). Experiments were performed in single-mixing mode as indicated. (i) Oxyferrous DHP B at a final concentration of 10 μM was mixed with 2.5–25 equiv of H_2O_2 , and (ii) a solution containing a final oxyferrous DHP B concentration of 10 μM and 1–30 equiv of TCP was reacted with 2.5–25 equiv of H_2O_2 . Experiments were performed in double-mixing mode using an aging line prior to the second mixing step. The design of the experiments allowed for the mixing of oxyferrous DHP B containing 1 equiv of TCP with 2.5 equiv of H_2O_2 for various aging times, followed by the second mix with an additional

2.5–25 equiv of TCP. (i) Oxyferrous DHP B + TCP (1 equiv) + H_2O_2 (2.5 equiv) \rightarrow delay \rightarrow TCP (2.5–25 equiv). All data were evaluated using the Specfit Global Analysis System software package (Spectrum Software Associates) and fit to exponential functions as either one-step, two-species or two-step, three-species irreversible mechanisms, where applicable. Kinetics data were baseline corrected using the Specfit autozero function.

Benchtop Optical Measurements. UV–visible absorption spectra were recorded at room temperature. Oxyferrous DHP B (10 μM) was incubated with 1, 15, or 30 equiv of TCP in a 100 mM KP_i buffer solution at pH 8. Reaction was initiated by addition of H_2O_2 (2.5–25 equiv). Spectra were recorded every 0.1 min for a period of 5 min.

Preparation of Reaction Intermediates by Freeze-Quench Methods. Rapid freeze-quench experiments were performed with a Bio-Logic SFM 400 freeze-quench apparatus by mixing a 50 μM oxyferrous DHP B solution (final concentration) containing 2,4,6-trichlorophenol (1 and 15 equiv) with a 10-fold excess of H_2O_2 in 100 mM KP_i (pH 8) at 25 °C. A standard 4 mm outside diameter quartz EPR tube was connected to a Teflon funnel, and both the tube and the funnel were completely immersed in an isopentane bath at -110 °C. The reactions were quenched when the mixtures were sprayed them into the cold isopentane, and the frozen material so obtained was packed at the bottom of the quartz tube using a packing rod equipped with a Teflon plunger. In this manner, a packing factor of $60 \pm 2\%$ was consistently achieved. Reaction times were as follows: 100 ms, 1 s, and 30 s (1 equiv of TCP) or 100 ms and 10 s (15 equiv of TCP). Samples were then transferred to a liquid nitrogen storage dewar until they were analyzed. Up to 200 individual scans were averaged to achieve a sufficient signal-to-noise ratio.

X-Band EPR Spectroscopy. EPR spectra were recorded with an X-band (9 GHz) Varian E-9 EPR spectrometer (Varian). A standard 4 mm outside diameter quartz EPR tube containing the sample was placed into a quartz finger dewar insert filled with liquid nitrogen. The temperature of the samples was maintained at 77 K for the duration of the data acquisition, which required periodic refilling of the dewar because of the evaporation of the liquid nitrogen during longer acquisition runs. The typical spectrometer settings were as follows: field sweep, 200 G; scan rate, 3.33 G/s; modulation frequency, 100 kHz; modulation amplitude, 4.0 G; microwave power, 2 mW. The exact resonant frequency of each EPR experiment was measured with an EIP-578 (PhaseMatrix, San Jose, CA) in-line microwave frequency counter.

TCP Radical Spin Trapping Experiments. A solution (500 μL) of 5.0 mM TCP in a 1:1 DMF/100 mM KP_i mixture (pH 7) with 10 mM H_2O_2 was added over a period of 3 h using a microsyringe pump to 500 μL of a solution of DIPPMO (1.5 mM) and ferric or oxyferrous DHP B (60 μM), or horseradish peroxidase. For the ³¹P NMR samples, 300 μL of the reaction mixture was added to 100 μL of D_2O with chromium chloride as a relaxation agent and trimethyl phosphate as the internal standard.³⁷

RESULTS

Formation and UV–Visible Characterization of Oxyferrous DHP B. Oxyferrous DHP was generated using different reducing agents (see the Supporting Information). Addition of sodium dithionite ($\text{Na}_2\text{S}_2\text{O}_4$, 25 equiv) (Figure SD1A of the Supporting Information, $E^{o'}$ $\sim -660 \text{ mV}^{38}$) or tris(2-carboxyethyl)phosphine (TCEP, 1 mM) (Figure SD1B of the Supporting

Table 1. Kinetics Data for the Oxidative Dehalogenation Reaction of TFP, TCP, and TBP (150 μM) As Catalyzed by 0.5 μM Oxyferrous DHP B in the Presence of Varying Concentrations of H_2O_2 at pH 7

cosubstrate	$K_m^{\text{H}_2\text{O}_2}$ (μM)	k_{cat} (s^{-1})	$k_{\text{cat}}/K_m^{\text{H}_2\text{O}_2}$ ($\mu\text{M}^{-1} \text{s}^{-1}$)
TFP	69 \pm 12	not available	not available
TCP ^a	35 \pm 6	1.17 \pm 0.05	0.034
TBP	17 \pm 1	0.70 \pm 0.04	0.041

^a Obtained from ref 26.

Information, $E^{\text{of}} \sim -0.05 \text{ V}^{39}$) to ferric DHP [UV-visible features at 407 (Soret), 504, 538, and 635 nm] resulted in the clean formation of oxyferrous DHP [UV-visible features at 417–418 (Soret), 543, and 578 nm], which was found to be relatively stable under the conditions examined. Interestingly, while TCEP is able to reduce DHP B [$E^{\text{of}}(\text{Fe}^{\text{III}}/\text{Fe}^{\text{II}}) = 0.206 \text{ V}$ vs NHE²⁶], it is not able to reduce HhMb [$E^{\text{of}}(\text{Fe}^{\text{III}}/\text{Fe}^{\text{II}}) = 0.046 \text{ V}$ vs NHE⁴⁰], highlighting an electrochemical difference between these two globins with potential functional implications that have been discussed previously.²⁶

Recombinant oxyferrous DHP B was also obtained by treatment of ferric DHP B with ascorbic acid ($E^{\text{of}} = 0.058 \text{ V}$ vs SHE, pH 7⁴¹), followed by the use of size exclusion chromatography to remove excess ascorbic acid. The electronic absorption spectra of oxyferrous DHP B prepared in this manner at pH 8 in the presence and absence of TCP are presented in Figure SD2 of the Supporting Information. Other than the absorption maxima at 245 and 312 nm observed for TCP, its addition did not alter the spectral features of the oxyferrous species. Oxyferrous DHP exhibited a typical spectrum of 6cLS ferrous heme with a Soret absorption band at 417 nm and the corresponding visible bands at 542 and 578 nm as noted previously.^{10,17,26,28} The ferric DHP B spectrum at this pH value was the spectrum of a hydroxide-bound heme protein as previously reported.¹⁶

Enzymatic Activity of Oxyferrous DHP B. The hydrogen peroxide-dependent oxidative dehalogenation of 2,4,6-tribromophenol and 2,4,6-trifluorophenol as catalyzed by oxyferrous DHP B at pH 7 was monitored by UV-visible spectroscopy, and the kinetic parameters (k_{cat} , K_m , and k_{cat}/K_m) determined as a function of TXP cosubstrate are listed in Table 1 after the experimental data had been analyzed using Michaelis–Menten kinetics with the method of initial rates. The reaction mixture yielded the corresponding 2,6-dihalo-1,4-benzoquinone (DXQ) products, as expected, when reactions were initiated upon the addition of H_2O_2 . Both enzyme and TXP cosubstrate concentrations were held constant, while H_2O_2 concentrations were varied. The known molar absorptivity of TBP at pH 7 was utilized to compute $d[S]/dt$ to obtain the resulting k_{cat} value for the reaction of this cosubstrate. As we have noted before for TFP,²⁶ neither $-d[S]/dt$ nor $d[P]/dt$ was determined as the absorption maximum for the TFP cosubstrate ($\lambda_{\text{max}} = 330 \text{ nm}$) underwent a shift during catalytic turnover, and the molar absorptivity of the DFQ product is unknown. Consequently, the corresponding k_{cat} value for TFP oxidation could not be determined by these means.

In agreement with our previous observations, the oxyferrous DHP B activity observed for TBP, TCP, and TFP was not significantly different from the enzymatic activity of the ferric enzyme.^{10,26} These results were expected on the basis of our proposed mechanism (vide infra) and that of Dawson and co-workers,²⁸ as both mechanisms invoke the ferric form during substrate turnover.

Stopped-Flow UV-Visible Characterization of DHP B Compound II. Formation of high-valent iron-oxo intermediates generated from the reaction of oxyferrous DHP B with hydrogen peroxide was investigated by single-mixing stopped-flow UV-visible spectroscopy at pH 8. When oxyferrous DHP B species [UV-visible features at 418 (Soret), 541, and 577 nm] were rapidly mixed (2 ms) with a 10- or 25-fold excess (Figure SD3 of the Supporting Information) of H_2O_2 , no intermediates were observed over the 85 s observation period, but a slight decrease in Soret band intensity was noted. Dawson and co-workers have reported that oxyferrous DHP A converts to Compound RH in the presence of a 10-fold excess of H_2O_2 ,²⁸ with this chemistry occurring on a reaction time scale of 2000 s, which may explain the minor spectral changes observed on the 85 s time scale employed in this work. We used other conditions to evaluate the reproducibility of these results with several reaction modifications, including varying the H_2O_2 concentration and pH (6–8) and using different ways to form the oxyferrous species. Under all conditions examined, the oxyferrous form was not reactive with H_2O_2 as the oxidant within the time scale being used (data not shown).

However, when the oxyferrous DHP B solution was incubated with at least 1 equiv of TCP as the cosubstrate prior to being rapidly mixed with 10 equiv of H_2O_2 , substantial spectral changes were observed (Figure 1). The oxyferrous form converted to a species whose spectral features [UV-visible features at 420 (Soret), 546, and 588 nm] closely resembled that of a ferryl-containing intermediate (e.g., Compound II or ES). The assignment of the DHP B intermediate observed here to that of a ferryl-containing species is based upon our previous identification of such reaction intermediates in DHP,^{10,16,19,26,42} as well as the spectroscopic properties of other Fe(IV)-oxo species commonly found in typical peroxidases. Myoglobin^{43,44} and hemoglobin^{45,46} both exhibit similar red-shifted Soret features and have visible bands that appear generally at 540–545 and 580–590 nm for their respective ferryl heme intermediates. It is also important to note that Dawson and co-workers²⁸ observed a similar intermediate (under slightly different reaction conditions) that they attributed to either Compound ES or II, each of which is a ferryl-containing species. Assignment of this species as a traditional Compound I intermediate was ruled out because of a lack of hypochromicity (large decrease in the Soret band intensity) and the absence of a strong red shift of the Soret band that is typical for an iron(IV)-oxo porphyrin π -cation radical,^{47–49} whereas Compound 0 (ferric-hydroperoxide) was also ruled out because of time scale considerations^{50,51} and the lack of an observed hyperporphyrin spectrum.^{52,53} As Compound ES and Compound II, both ferryl-containing intermediates, cannot be distinguished by UV-visible spectroscopy, our assignment for the intermediate described here as Compound II was based upon the results of our EPR spectroscopic study (vide infra).

The experimental values of k_{obs} for Compound II formation (Scheme 1, step i) varied linearly with TCP in the range of 1–30 molar equiv. From this dependence, the bimolecular rate constant was determined to be $(1.60 \pm 0.14) \times 10^3 \text{ M}^{-1} \text{ s}^{-1}$ (Figure SD4 of the Supporting Information). When 1 equiv of TCP was employed, the formation of Compound II was observed over the 85 s observation period without conversion or decay to either the ferric enzyme or Compound RH (the decay product of Compound ES in the absence of TXP). When the concentration of TCP was increased to 15 equiv versus that of the enzyme (10-fold excess of H_2O_2 maintained), a partial conversion of the Compound

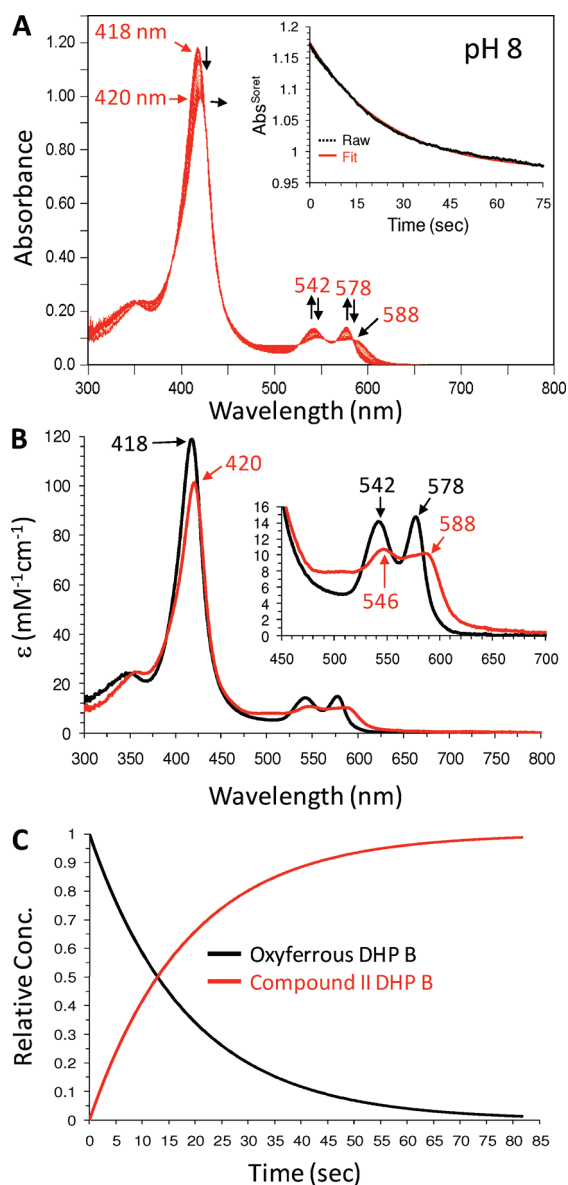


Figure 1. (A) Stopped-flow UV–visible spectroscopic monitoring of the reaction (900 scans, 85 s) between oxyferrous DHP B (10 μM) containing 1 equiv of TCP (10 μM) and a 10-fold excess of H_2O_2 at pH 8. (B) Calculated UV–visible spectra for both oxyferrous (black) and Compound II (red). The rapid-scanning data from panel A were fit to a one-step, two-species sequential irreversible model using Specfit global analysis software. (C) Relative concentration profile determined from the three-component fit used in panel B.

II intermediate to ferric DHP B was noted (data not shown), which was more clearly observed at 30 equiv of TCP (Figure SD5 of the Supporting Information), suggesting that TCP is a competent reducing agent for Compound II.

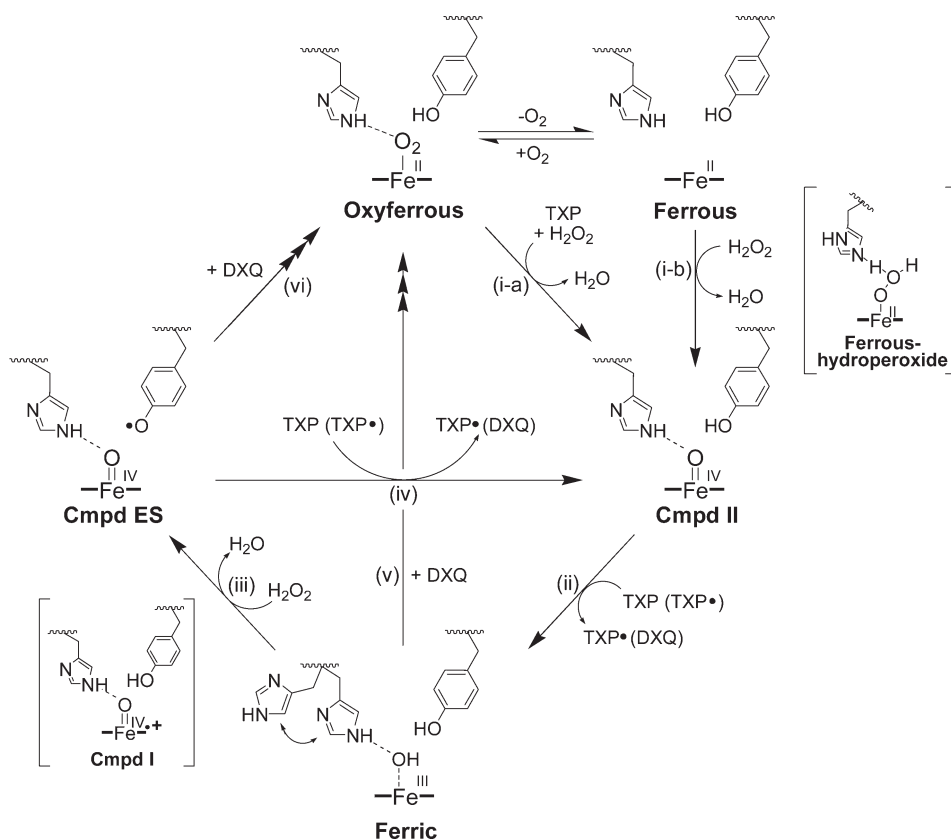
Several differences between the reactivity of Compound II and that of Compound ES are notable. First, the bimolecular rate constant for the formation of Compound II [Scheme 1, step i; $(1.60 \pm 0.14) \times 10^3 \text{ M}^{-1} \text{ s}^{-1}$] was significantly slower than that for formation of Compound ES (Scheme 1, step iii; $\sim 5.1 \times 10^4 \text{ M}^{-1} \text{ s}^{-1}$) when that latter species was generated from the ferric enzyme in the absence of TCP at pH 8 (Figure SD6 of the Supporting Information). Second, the reaction of ferric DHP B

incubated with 30 equiv of TCP and reacted with a 10-fold excess of H_2O_2 did not generate an observable Compound ES intermediate,²⁶ a result that was attributed to the rapid in situ reduction of the Compound ES species in the presence of TCP. However, our results here demonstrate that Compound II is significantly less reactive than Compound ES, as the reaction of oxyferrous DHP B incubated with 30 equiv of TCP with a 10-fold excess of H_2O_2 did yield a metastable [~ 15 s (Figure SD6 of the Supporting Information)] Compound II species prior to its reduction to the ferric enzyme.

To further investigate the reactivity of DHP B Compound II, sequential double-mixing stopped-flow studies were employed to monitor the reaction of preformed Compound II with TCP substrate by UV–visible spectroscopy (Figure SD7 of the Supporting Information). Oxyferrous DHP B containing 1 equiv of TCP was reacted with 2.5 molar equiv of H_2O_2 at pH 8, incubated for 85 s to allow for the maximal accumulation of Compound II, and subsequently mixed with an additional 2.5 equiv of TCP (Figure SD7A), 10 equiv (Figure SD7B), and 25 molar equiv of TCP (Figure SD7C), which resulted in the regeneration of ferric DHP B. The disappearance of Compound II (Scheme 1, step ii) and the formation of the ferric enzyme were linearly dependent on the concentration of TCP cosubstrate, yielding a bimolecular rate constant of $(4.1 \pm 0.3) \times 10^2 \text{ M}^{-1} \text{ s}^{-1}$ (Figure SD7D). At the highest concentration of TCP investigated [25 equiv (Figure SD7C)], the ferric form of the enzyme was further found to partially convert to oxyferrous DHP because of the presence of DCQ generated from the reaction of Compound II with TCP, in accordance with the known reactivity of ferric DHP B with DCQ.²⁶

Characterization of Compound II by EPR. Rapid-freeze-quench methods were employed to stabilize the ferryl intermediate observed in the reaction described above for subsequent characterization by continuous wave (CW) EPR spectroscopy. Specifically, X-band EPR spectra at various quench times (100 ms, 1 s, and 30 s) were obtained for the reaction of oxyferrous DHP B with a 10-fold excess of H_2O_2 in the presence of 1 equiv of TCP, thereby generating the putative Compound II intermediate. No detectable EPR signal was observed (Figure 2), indicating that no protein radical was present. For comparison, and as a control for verifying the experimental and spectroscopic apparatus, the EPR signal of Compound ES that resulted from the rapid mixing (500 ms) of ferric DHP B with 10 equiv of H_2O_2 at pH 8 (generated side by side with the oxyferrous reaction samples) is also shown. As previously reported, the free radical concentration in Compound ES is nearly quantitative with respect to the enzyme concentration (~ 0.93 spin/heme) in DHP.⁵⁴ As the EPR spectroscopic method presented here provides an unambiguous means of differentiating between the two ferryl-containing intermediates, Compound ES and Compound II, our spectroscopic data unequivocally rule out the intermediate observed above in the stopped-flow studies as Compound ES. The lack of a spectral signal obtained here strongly suggests either a diamagnetic or even-spin species, the latter being consistent with the assignment of Compound II as the intermediate generated in the reaction of oxyferrous DHP B and hydrogen peroxide in the presence of TCP.

To eliminate the possible interpretation that the lack of an observed radical signal was due to a Compound ES intermediate that was rapidly quenched by TCP, we employed RFQ-EPR spectroscopy to investigate the reaction of a 10-fold excess of H_2O_2 with ferric DHP B preincubated with 1 or 1.2 equiv of TCP

Scheme 1. Proposed Catalytic Cycle for (De)oxyferrous Dehaloperoxidase B^a


^a Adapted from ref 26. The pathways forming Compounds RH and P₄₂₆, as well as monohalophenol inhibition, have been omitted for the sake of clarity.

at a freeze-quench time of 100 ms (pH 8). Under these conditions, a radical signal was observed (Figure SD8 of the Supporting Information). Although the radical intensity in the presence of TCP was $\sim 10\%$ (0.09 spin/heme) of that of Compound ES itself in the absence of TCP, and the shape of the signal differed as well, the result of an observable radical formed under these conditions contrasts markedly with the lack of a radical observed from the reaction of oxyferrous DHP B with a 10-fold excess of H₂O₂ in the presence of 1 equiv of TCP. Thus, we exclude the possibility that the mechanism of DHP proceeds through a ferric state that yields a Compound ES species whose amino acid radical is quickly quenched by the TCP cosubstrate.

H₂O₂ Reactivity of Ferrous DHP B. The reactivity of ferrous DHP B with H₂O₂ was investigated using UV–visible spectroscopy under anaerobic conditions to prevent the formation of the oxyferrous species upon oxygen binding to the reduced enzyme. The UV–visible spectra were monitored inside a glovebox using a fiber optic dip probe. Because of the poor signal-to-noise ratio of the fiber optic setup, two enzyme concentrations, 10 and 50 μM , were employed for the data in Figure 3 to provide resolution of both the Soret and visible bands (as shown in the inset), respectively. The reduced enzyme was obtained from the titration of ferric DHP B with substoichiometric additions of sodium dithionite until fully formed [UV–vis features at 432 (Soret) and 558 nm^{17,26}] (Figure SD9 of the Supporting Information). Ferrous DHP B (10 or 50 μM) thus generated was mixed with excess H₂O₂ (2.5–10 equiv), and the resulting changes in the electronic absorption spectrum were recorded immediately after mixing (~ 2 –3 s). Overall, two intermediates were observed

prior to the formation of the final product (as either ferric DHP B or Compound RH, depending upon the reaction conditions employed). Ferrous DHP B first converted to a new species [UV–vis features at ~ 421 –423 (Soret), 488, and 505 (sh) nm; $k_{\text{obs}} > 0.6 \text{ s}^{-1}$] (Figure 3 and Figure SD10 of the Supporting Information), which was found to be unstable, and interconverted ($k_{\text{obs}} \sim 0.036 \text{ s}^{-1}$) to a second intermediate whose spectral features [UV–vis features at 420 (Soret), 546, and 586 nm] we attribute to the ferryl-containing intermediate Compound II on the basis of (i) spectral similarity to other ferryl-hemes (vide supra), (ii) the results of our EPR spectroscopic study (vide supra), and (iii) the known reactivity of ferrous heme proteins with H₂O₂ (see Discussion). The observed amount of this unknown intermediate appeared to be proportional to the amount of hydrogen peroxide that was initially reacted with ferrous DHP B (Figure 3), although the temporal resolution of the anaerobic dip probe/UV–visible benchtop spectrometer did not allow a quantitative assessment to be made. The reaction was repeated at a reduced temperature ($\sim 4 \text{ }^\circ\text{C}$) to stabilize the intermediate and obtain the spectrum shown in Figure 4. The visible bands [488 and 505 (sh) nm] clearly are distinct from those of ferric DHP B, Compound I or II/ES, and ferrous DHP B in terms of both absorption maxima and molar absorptivity. The Soret band (~ 421 –423 nm) is also distinct when compared to that of the ferrous (432 nm) or ferric (410 nm) form of the enzyme at this pH. Overall, the UV–visible spectroscopic data suggest the presence of an intermediate prior to the formation of Compound II, with the latter peroxidase-active species being formed from the ferrous enzyme in the absence of TCP. Addition

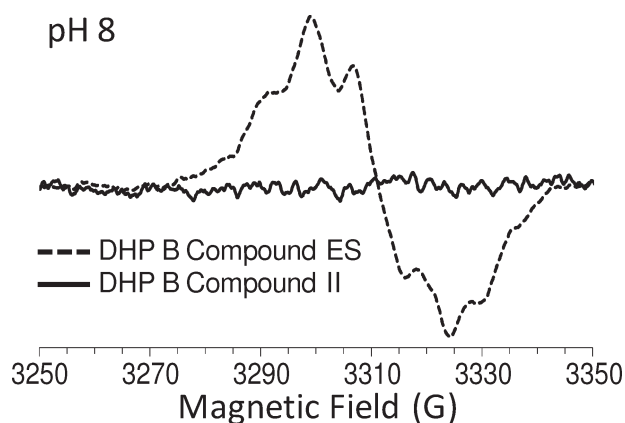


Figure 2. EPR spectrum of DHP B Compound II at a freeze-quench time of 100 ms (pH 8). Data collected at 1 and 30 s quench times for DHP B Compound II similarly showed no signal. For the purpose of comparison, the EPR spectrum of Compound ES is also shown. Rapid-freeze-quench samples were prepared via the reaction of oxyferrous DHP B ($50 \mu\text{M}$ final) containing 1 equiv of TCP with a 10-fold excess of H_2O_2 at 25°C and rapidly frozen in an isopentane slurry.

of TCP (10 equiv) to the Compound II intermediate formed here in the absence of cosubstrate yielded the ferric state of the enzyme as expected (data not shown).

In the presence of 1 equiv of TCP, the reaction of ferrous DHP B with hydrogen peroxide was qualitatively similar to that described above for the reaction in the absence of trihalophenol in that the formation of an intermediate was observed prior to the identification of Compound II (Figure SD11 of the Supporting Information). Again, this intermediate interconverted to form Compound II [UV-vis features at 420 (Soret), 546, and 586 nm], but the process was ~ 5 -fold faster than when TCP was absent. Under the conditions examined, Compound II was stable for the duration of the 60 s observation window, a marked contrast to the instability of Compound ES under similar conditions.^{10,26} However, when the TCP concentration in the reaction mixture was increased to 30 equiv, the Compound II intermediate converted to ferric DHP B (Figure SD12 of the Supporting Information), with a concomitant decrease in the TCP absorbance (312 nm) that was proportional to the amount of hydrogen peroxide initially reacted (Figure SD12A of the Supporting Information, 2.5 equiv of H_2O_2 ; Figure SD12B of the Supporting Information, 10 equiv of H_2O_2). The TCP-dependent reactivity of Compound II observed here was consistent with that noted for the reaction of oxyferrous DHP B with hydrogen peroxide from our stopped-flow study (*vide supra*).

Reactivity Studies of Oxyferrous DHP B. The reaction of oxyferrous DHP B ($10 \mu\text{M}$) with hydrogen peroxide (2.5, 10, and 25 equiv) in the presence of TCP cosubstrate yielding DCQ was further explored by UV-visible spectroscopy. No reaction was observed upon the addition of $100 \mu\text{M}$ H_2O_2 to a solution of oxyferrous DHP B containing a substoichiometric amount of TCP [0.5 equiv (data not shown)]. As such, the TCP concentration was varied over a range of 10, 150, and $300 \mu\text{M}$ [1–30 equiv (Figures SD13–SD15 of the Supporting Information)] to evaluate the effect of cosubstrate on Compound II formation and reactivity. With 1 equiv of TCP, the DHP B Compound II intermediate was found to be stable over the reaction time of 60 s (Figure SD13 of the Supporting Information). Neither TCP loss (312 nm) nor DCQ formation (274 nm) could be observed

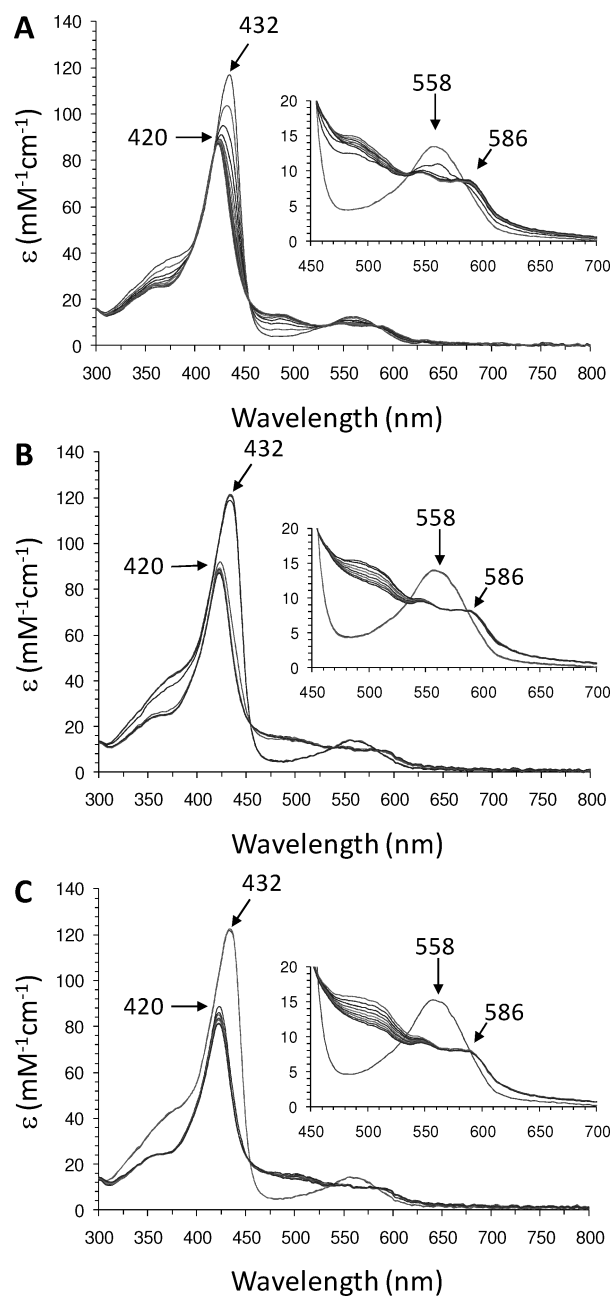


Figure 3. UV-visible spectroscopic monitoring (10 scans, 0.1 min interval/scan, 60 s total) of the reaction between ferrous DHP B ($10 \mu\text{M}$) and (A) 2.5, (B) 10, or (C) 25 equiv of H_2O_2 yielding Compound II at pH 8. The insets show results for the same experimental conditions described above except that the ferrous DHP B concentration was $50 \mu\text{M}$.

when only 1 equiv of TCP was initially reacted. As observed in the stopped-flow study (*vide supra*), when the amount of TCP (15–30 equiv) greatly exceeded that of H_2O_2 , the ferryl-containing intermediate converted to a species whose spectral features matched those of ferric DHP B (Figures SD14 and SD15 of the Supporting Information), concomitant with TCP loss and DCQ formation, the extent for both being well-correlated with the amount of H_2O_2 initially employed in the reaction. Reaction conditions that generated both ferric DHP B and a relatively large amount of DCQ [i.e., $300 \mu\text{M}$ TCP and $100 \mu\text{M}$ H_2O_2 (Figure

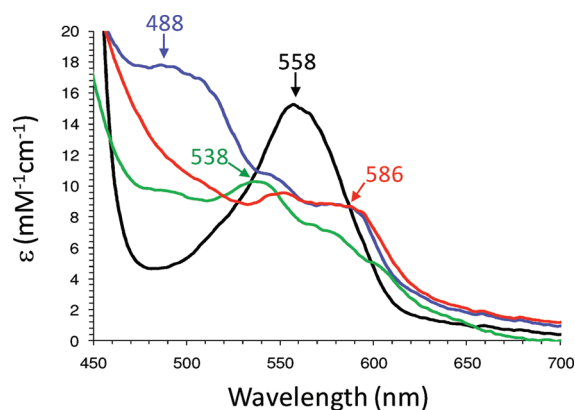


Figure 4. Comparison of the visible spectroscopic features of ferrous DHP B (10 μM , black), ferric DHP B (green), Compound II (red), and the putative ferrous-hydroperoxide intermediate (blue) that was formed prior to Compound II in 100 mM KP_i (pH 8) at 4 $^\circ\text{C}$.

SD15B of the Supporting Information)] exhibited re-formation of the oxyferrous state at longer reaction times [5 min (data not shown)]. This observation was consistent with our previous report that incubation of the ferric form of the enzyme with DCQ generates oxyferrous DHP B.²⁶ At higher concentrations of H_2O_2 , bleaching of the heme cofactor was noted. The apparent increase in the baseline between 450 and 550 nm when high concentrations of DCQ are formed may be attributable to the formation of 2,6-dichloro-3-hydroxy-1,4-benzoquinone (DCHB) as a secondary product ($\lambda_{\text{max}} = 524 \text{ nm}$; $\epsilon = 2530 \pm 60 \text{ M}^{-1} \text{ cm}^{-1}$).^{55,56}

Trapping of TCP Radicals during Enzymatic Turnover.

TCP radicals generated from the reaction of ferric or oxyferrous DHP B (30 μM) and H_2O_2 (5 mM) in the presence of 1.25 mM TCP at pH 7 were trapped using the radical trap 5-diisopropoxyphosphoryl-5-methyl-1-pyrroline-*N*-oxide (DIPPMO). As an alternative to traditional EPR spectroscopic methods, the results were analyzed by ^{31}P NMR spectroscopy as previously described.³⁷ DIPPMO alone exhibited a resonance at 22.2 ppm (Figure SD16A of the Supporting Information). The ^{31}P NMR spectra recorded after the reaction employing either ferric (Figure SD16B of the Supporting Information) or oxyferrous DHP B (Figure SD16C of the Supporting Information) both exhibited two peaks at 22.2 and 25.1 ppm, which correspond to the native spin trap signal and the covalent adduct of TCP-DIPPMO, respectively. These NMR spectroscopic results for DHP B were indistinguishable from the previous identification [and reconfirmed here as a control (Figure SD16D of the Supporting Information)] of TCP radicals generated from the reaction of horseradish peroxidase with H_2O_2 in the presence of TCP³⁷ and provide unequivocal evidence of the formation of TCP radicals that have been postulated to form during dehaloperoxidase turnover.^{21,26}

DISCUSSION

As both an oxygen transport globin and a peroxidase, dehaloperoxidase from the terebellid polychaete *A. ornata* possesses two inherent functions that occur at a single heme active site. Given that reversible oxygen binding is only mediated via a ferrous heme in globins, and that peroxidase activity is initiated from ferric centers and to the exclusion of the oxyferrous oxidation state from the peroxidase cycle, the bifunctional nature of DHP as a globin peroxidase appears to be at odds with the

traditional starting oxidation state for each individual activity. Our understanding of how the enzyme rectifies this apparent paradox, wherein the peroxidase-active ferric DHP state can be converted to the oxygen-binding ferrous form, or the reverse, wherein oxyferrous DHP is activated toward peroxidase function, is still lacking. Thus, as the means of resolving this paradox, the primary focus of this report is to provide the details of dehaloperoxidase chemistry that have yet to be reported for the deoxyferrous state of the enzyme and to augment those with additional studies of oxyferrous DHP.

The activity studies presented here further demonstrate that dehaloperoxidase B is able to catalyze the oxidative dehalogenation of 2,4,6-trihalogenated phenols to their corresponding 2,6-dihalo-1,4-benzoquinones in the presence of hydrogen peroxide when the catalytic cycle is initiated from the oxyferrous state. This is critically important given that the oxyferrous state is normally a catalytically incompetent species for monofunctional peroxidases⁵⁷ and represents a partial solution to the aforementioned paradox. As it is possible that dehaloperoxidase may have evolved its peroxidase function to begin from the oxyferrous state, which is the normal oxidation state for this hemoglobin in *A. ornata*, the reaction of oxyferrous DHP with hydrogen peroxide was further investigated using stopped-flow UV-visible spectroscopy. In the presence of as little as 1 equiv of TCP cosubstrate, the first intermediate observed exhibited spectral features that matched those of a ferryl-containing species that lacked a porphyrin π -cation radical,¹⁰ suggestive of the formation of either Compound ES or Compound II. However, Compound ES was ruled out on the basis of electron counting, as it is oxidized by three electrons with respect to the starting ferrous oxidation state, and hydrogen peroxide is only a two-electron oxidant when cleaved heterolytically. Furthermore, RFQ-CW-EPR spectroscopic studies presented here also ruled out this intermediate as Compound ES, as the presence of a protein radical was not observed, consistent with the formulation of the ferryl-containing intermediate as DHP B Compound II.

When oxyferrous DHP was reacted under conditions where the TCP concentration was greater than the H_2O_2 concentration, it was observed that Compound II converted to the ferric form of the enzyme, concomitant with TCP loss and DCQ formation. Sequential double-mixing stopped-flow studies demonstrated that DHP B Compound II was directly capable of oxidizing TCP. These results were consistent with TCP serving as a one-electron reducing agent. Dawson and co-workers²¹ recently reported evidence supporting a peroxidase cycle for DHP A involving two sequential one-electron oxidations of TCP to yield DCQ when preformed Compound ES was employed (presumably via a transiently formed Compound II species), and it appears that TCP here is serving a similar function in terms of reducing Compound II to the ferric state. Ferric DHP B was not the final “resting” state of the enzyme, however, as experimental conditions that favored the formation of DCQ also led to the regeneration of the starting oxyferrous DHP B species. We attribute this to the previously characterized reaction between ferric DHP B and DCQ,²⁶ which was shown to form oxyferrous DHP B. The unusually high reduction potential of 206 mV for a peroxidase likely favors reduction of the ferric heme and formation of oxyferrous DHP B in the presence of DCQ.

In light of the spectroscopic and biochemical findings presented here, we propose the following updated mechanism for the *in vitro* peroxide-dependent oxidation of trihalophenol as catalyzed by DHP B from *A. ornata* (Scheme 1). In the presence

of trihalophenol, (de)oxyferrous DHP B reacts with H_2O_2 to form the peroxidase-active species Compound II (step i-a or i-b), which is subsequently reduced in the presence of excess TXP to the ferric enzyme (step ii). The ferric enzyme can proceed along a traditional peroxidase reaction pathway, reacting with hydrogen peroxide to generate Compound ES via a transiently formed Compound I species (step iii) and returning to the ferric state via two consecutive one-electron reduction steps as postulated by Dawson and co-workers²¹ (steps iv and ii). Dihaloquinone can be formed from either two consecutive one-electron oxidations of TXP (via a TXP radical) or the disproportionation of TXP radicals. The DXQ product thus formed, either because of its inherent instability or as an alternative cosubstrate for the enzyme, leads to the reduction of the ferric state to the ferrous state, generating oxyferrous DHP B in the presence of dioxygen (step v). Alternatively, Compound ES may directly react with DCQ as a cosubstrate, leading to the generation of the (de)oxyferrous species (step vi). The proposed mechanism therefore resolves the dehaloperoxidase paradox in which the bifunctional nature of a globin peroxidase appears to be at odds with the traditional starting oxidation state for each individual activity. Namely, (de)oxyferrous DHP B is a catalytically competent state for initiating a peroxidase catalytic cycle and is the first such example that has a relevant biological function. Moreover, as discussed previously²⁶ and noted here in additional detail, dihaloquinone generated from the peroxidase cycle is itself a substrate for both ferric and Compound ES DHP B, leading to formation of oxyferrous DHP B. Thus, the product of the peroxidase cycle regenerates the globin-active species, which is also a viable oxidation state for initiating peroxidase chemistry. Taken together, these two reactivities observed here highlight the unique chemistry of dehaloperoxidase that allows both globin and peroxidase discrete functions from what appears to be a limited set of resources.

Interestingly, in the absence of TCP, oxyferrous DHP B was unreactive toward hydrogen peroxide with respect to the formation of observable high-valent iron–oxo intermediates (i.e., Compound II), and therefore, a role for trihalophenol needs to be postulated that is consistent with the mechanism described above. Dawson and co-workers have suggested that the observed conversion of oxyferrous DHP to Compound II or ES was due to the presence of a trace amount of ferric DHP that undergoes a traditional peroxidase cycle, thereby generating TCP radicals that oxidize the bulk oxyferrous DHP to the ferric enzyme.²⁸ Subsequent reaction of the resulting ferric DHP with hydrogen peroxide generates the observed ferryl-containing species. In that work, the typical reaction conditions employed an excess of TCP with respect to H_2O_2 . Although precedent for the oxyferrous to ferric conversion as catalyzed by substrate radicals has been demonstrated for lignin peroxidase, the reaction conditions employed in our RFQ-EPR spectroscopic study and stoichiometric considerations argue against this mechanism. Specifically, 10 equiv of H_2O_2 was reacted with oxyferrous DHP B in the presence of 1 equiv of TCP. Assuming trace ferric DHP B initially reacted to generate TCP radicals, which then oxidized oxyferrous DHP B to the ferric form (thereby regenerating TCP in the process), 0.5 equiv of hydrogen peroxide would have then been consumed, leaving 9.5 equiv of H_2O_2 to subsequently react with the ferric enzyme and TCP in solution (1 equiv each). This reaction would generate DHP B Compound ES in situ, a two-electron oxidant that has been shown to react rapidly with TCP to yield DCQ (1 equiv) and the ferric enzyme.²⁶ The ferric

enzyme would then react with the remaining H_2O_2 , re-forming Compound ES, whose subsequent reaction with DCQ is slow enough to have allowed identification of the amino acid radical of this intermediate by RFQ-EPR spectroscopy. As no protein radical was observed in our EPR spectroscopic study, we conclude that the observed oxyferrous reactivity yielding Compound II cannot be attributed to a mechanism invoking a transiently formed ferric state, and that the oxidation of oxyferrous DHP B via TCP radicals is unlikely under the reaction conditions examined ($[\text{H}_2\text{O}_2] > [\text{TCP}]$).

Thus, an alternative mechanism that involves trihalophenol binding, but not TXP radical formation, is needed to describe the reaction of oxyferrous DHP with hydrogen peroxide yielding Compound II. On the basis of our anaerobic studies, we suggest that the reaction of deoxyferrous DHP B with H_2O_2 is responsible for the formation of the observed Compound II intermediate and that trihalophenol binding plays a role in the activation of oxyferrous DHP to the deoxy state when hydrogen peroxide is present. Specifically, we have observed the formation of Compound II upon the reaction of deoxyferrous DHP B with hydrogen peroxide in the absence of trihalophenol. The conversion of deoxyferrous hemoproteins to Compound II in what is generally regarded as a single-step, two-electron oxidation has been noted and/or postulated in a number of other systems, including horseradish peroxidase,⁵⁸ leghemoglobin,⁵⁹ lactoperoxidase,^{60,61} myeloperoxidase,⁶² and KatG.⁶³ Importantly, none of aforementioned systems invoked substrate radicals as mechanistically relevant to account for their observed chemistry. Furthermore, the importance of this observation is also underscored by the *in vivo* role of dehaloperoxidase as an oxygen-transport protein, wherein the globin exists in both the oxy- and deoxyferrous states, and it is reasonable to surmise that the initiation of a peroxidase pathway should not be limited to only one of the two major states of a globin.

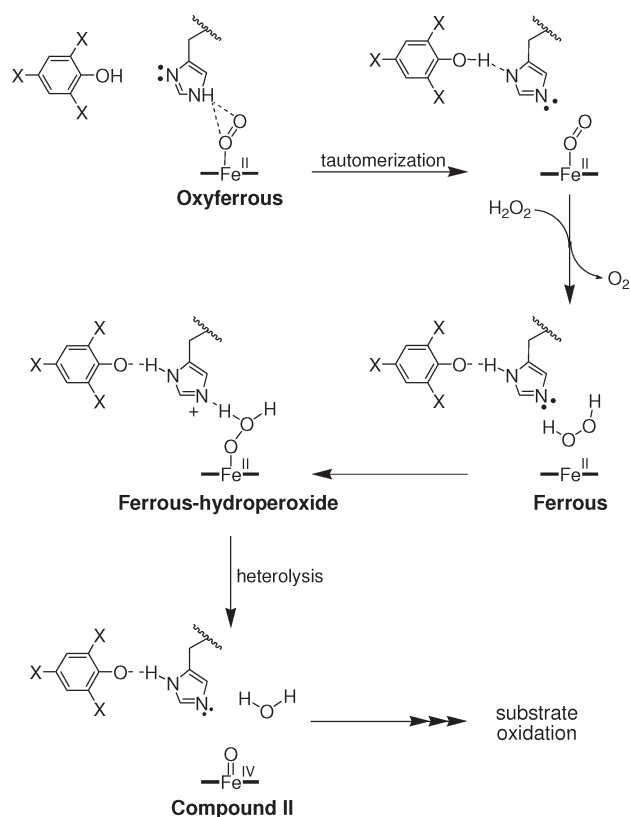
The reaction of deoxyferrous DHP B with hydrogen peroxide surprisingly revealed an intermediate that formed prior to the full formation of Compound II. The spectral features of this species did not match any for the known intermediates of dehaloperoxidase (e.g., Compounds I, II, ES, and III).^{10,26} One possibility is that this intermediate preliminarily represents the ferrous–hydroperoxide adduct that must form prior to heterolytic cleavage of the hydrogen peroxide that ultimately yields Compound II. The observation of the Fe(II)–OOH precursor prior to Compound II formation is analogous to the Compound 0 species, Fe(III)–OOH, that has been shown to form prior to Compound I in traditional heme chemistry.^{52,53,64–68} Typically, such ferric–hydroperoxide species are short-lived ($<200 \mu\text{s}$);⁶⁴ however, examples of peroxidase⁶⁹ and myoglobin mutants,⁶⁸ as well as native cytochrome c_{552} ,⁶⁵ that exhibit more reasonable lifetimes (milliseconds to seconds) have been reported, with the consensus opinion that the lack of a suitable proton donor in the hydrophobic heme cavities lowers the rate of heterolytic O–O bond cleavage, thereby stabilizing Compound 0. A similar argument can be posited to account for the relative stability of the putative ferrous–hydroperoxide intermediate of DHP B, as the distal histidine–heme distance in dehaloperoxidase (Fe–His $\text{N}^{\epsilon 2} = 5.5 \text{ \AA}$,³³ ferric DHP B, His⁵⁵ in the closed position) is intermediate between those found in globins (4.1–4.6 Å) and peroxidases (5.5–6.0 Å)^{29–32} and as such may not be ideally positioned to facilitate H_2O_2 heterolysis. Further, when TCP was present prior to the reaction of deoxyferrous DHP B with H_2O_2 , the stability of the Fe(II)–OOH intermediate was lowered, and

we surmise that the position of the distal histidine (and the nature of the tautomeric bonds of the imidazole ring) thus facilitates O–O bond cleavage when trihalophenol is bound. This is consistent with the postulate that both external and internal small-molecule binding sites may exist with regulatory implications linked to the conformation flexibility of the distal histidine, His⁵⁵, that may govern how DHP switches between its hemoglobin and peroxidase activities.^{11–13,33} An additional consideration that may contribute to the stability of the ferrous–hydroperoxide precursor is the very positive Fe(III)/Fe(II) reduction potential (~200 mV) of DHP.²⁶ Rather than the nearly ubiquitous Asp-His-Fe or Glu-His-Fe charge relays that are found in peroxidases and have been shown to impart a partially anionic character to the proximal histidine, dehaloperoxidase lacks such a catalytic triad. Instead, DHP possesses a proximal histidine that is in van der Waals contact with Met^{86,35} and vibrational studies have suggested the presence of a neutral proximal histidine that is unlikely to activate bound peroxide via a push effect.⁷⁰ Consequently, the lack of a push effect in DHP and a high reduction potential are two additional factors related to the presence of Met⁸⁶ that likely contribute to the stability of the putative Fe(II)–OOH species.

The lack of reactivity observed for oxyferrous DHP B may have a physiological role when trihalophenol cosubstrate is absent, preventing formation of Compound RH (with its attenuated dehaloperoxidase activity) when exposed to hydrogen peroxide for short reaction times (<60 s), and also minimizing the deleterious effects of unwanted peroxidase activity in the absence of a reducing substrate. In the case of the different reactivity observed for ferrous and oxyferrous DHP B in the absence of trihalophenol, it is likely that the bound oxygen molecule acts as an inhibitor of the reaction by blocking H₂O₂ from binding to the heme iron. As described by Alayash and co-workers⁷¹ for the reaction of oxyferrous swMb with hydrogen peroxide, the rate constant that describes the initial oxidation of the oxyferrous heme by hydrogen peroxide reflects the competition between the two ligands, O₂ and H₂O₂, for the ferrous iron. Under conditions with high H₂O₂ and low O₂ concentrations, the apparent rate of the oxyferrous reaction approaches that of the intrinsic rate constant for heterolytic cleavage of the bound peroxide, whereas under reaction conditions with high O₂ and low H₂O₂ concentrations, the rate is proportional to $K_{\text{H}_2\text{O}_2}/K_{\text{O}_2}$, the ratio of the binding constants of the two ligands. The kinetic observations by Dawson and co-workers for the reaction of oxyferrous DHP with hydrogen peroxide (TCP present),²⁸ when reinterpreted in light of our proposed mechanism of direct (de)oxyferrous oxidation to Compound II (Schemes 1 and 2), appear to be consistent with the kinetic scheme of Alayash and co-workers with respect to the observed lag times that were presented as evidence of the conversion of oxyferrous DHP to the ferric state via substrate radicals (generated from trace ferric DHP). However, further studies exploring both mechanistic interpretations will be necessary to fully elucidate the details of this process.

It is clear that trihalophenol binding triggers the activation of oxyferrous DHP B to Compound II in the presence of hydrogen peroxide. It has been suggested that His⁵⁵, which has been observed in distinct “open” and “closed” conformations, mediates displacement of O₂ from the heme in the presence of (tri)halophenol substrate, possibly serving as this trigger for peroxidase function.¹¹ Given this, and in light of the results described herein, we have considered the role of the distal histidine as being integral to the substrate-dependent activation of oxyferrous DHP B and propose the following mechanism for

Scheme 2. Proposed Tautomerization of the Distal Histidine in Oxyferrous DHP B upon Trihalophenol Binding^a



^a A direct interaction between His⁵⁵ and TXP is depicted; however, binding may occur elsewhere, leading to the proposed tautomerization. TXP binding may occur as the trihalophenolate.

the activation step of the dehaloperoxidase cycle (Scheme 2). When trihalophenol binds (possibly as trihalophenolate) to oxyferrous DHP, tautomerization of the distal His⁵⁵ occurs, forming a hydrogen bond between the His N^δ atom and the phenolic hydrogen of the cosubstrate and disrupting the hydrogen bond between the His N^{ε2} atom and the bound oxygen ligand that had stabilized the oxyferrous species. Evidence of the destabilization of oxyferrous DHP upon trihalophenol binding comes from Dawson and co-workers, who observed a 2.6-fold increase in the rate of autoxidation of the oxyferrous enzyme in the presence of TCP when compared to that in its absence.²⁸ The destabilized oxyferrous DHP is therefore activated for reaction with hydrogen peroxide, which displaces the now weakly bound oxygen ligand, generating the Fe(II)–OOH intermediate that was observed in the deoxyferrous studies. Heterolysis of this ferrous–hydroperoxide intermediate, facilitated by the tautomer that now positions the His N^{ε2} atom as a general base, yields Compound II, which can now initiate a peroxidase cycle as described in Scheme 1. It is important to note that although the trihalophenol binding site is believed to be external to the heme active site,^{11–13} it is not known whether bound TXP can directly interact with the distal histidine. Thus, tautomerization may result from a direct or indirect (allosteric) binding event, and this ambiguity is schematically represented in Scheme 2. There are several examples in the literature in which histidine tautomerization has played an important role during enzymatic function for both heme and

non-heme proteins. These include (i) human carbonic anhydrase II (hCAII), where the tautomers of His⁶⁴ (tautomeric equilibrium constant of 1.0) act as both a general acid and base, mediating the transfer of both protons and water molecules at a neutral pH with high efficiency,⁷² and (ii) myoglobin,^{73–79} where the distal histidine, His⁶⁴, has been postulated to play a role in the discrimination of oxygen versus CO binding. It is thought that entry of ligand into the heme pocket of Mb is controlled by the distal histidine gate, and hydrogen bond donation through the neutral N^oH tautomer of His⁶⁴ regulates oxygen affinity. In our system, we propose that TXP cosubstrate binding similarly affects the stability of the oxyferrous enzyme, allowing reaction with hydrogen peroxide and allowing the distal histidine to serve as the general base required for H₂O₂ heterolysis.

CONCLUSION

We have shown that the reaction of deoxyferrous DHP with hydrogen peroxide forms Compound II, a peroxidase active species, in the absence of trihalophenol. Literature precedent for other heme systems supports such a direct two-electron oxidation of the deoxyferrous heme without the need for invoking a ferric oxidation state that has been the traditional starting point for initiating the peroxidase catalytic cycle. Further, although not altogether excluding a role for substrate radicals in effecting an oxyferrous to Compound II conversion, the proposed mechanism suggests that substrate radicals need not be considered for this process to occur, and that a simple displacement of the bound oxygen ligand upon simultaneous trihalophenol and H₂O₂ binding suffices. We have also found preliminary evidence of a ferrous–hydroperoxide intermediate that forms prior to Compound II. Given the relative stability of this species, future studies will be directed toward its characterization and reactivity. When combined with the known DCQ-driven reduction of ferric DHP to the oxyferrous enzyme, the chemistry reported herein establishes oxyferrous DHP as both a starting and end point for peroxidase chemistry that maintains a globin-active center, resolves the oxidation state paradox of globin peroxidases, and improves our understanding of how this bifunctional enzyme is able to unite its two inherent functions in one system.

ASSOCIATED CONTENT

S Supporting Information. Methods for the preparation of oxyferrous DHP B from TCEP or sodium dithionite (Figure SD1), UV–visible spectra of oxyferrous DHP B in the presence and absence of TCP (Figure SD2), stopped-flow UV–visible spectroscopic monitoring of the reaction between oxyferrous DHP B and a 10-fold excess of H₂O₂ (Figure SD3), dependence of *k*_{obs} on TCP concentration for the formation of DHP B Compound II (Figure SD4), stopped-flow UV–visible spectroscopic monitoring of the reaction between oxyferrous DHP B containing 30 equiv of TCP and a 10-fold excess of H₂O₂ (Figure SD5), stopped-flow UV–visible spectroscopic monitoring of the reaction between ferric DHP B and a 10-fold excess of H₂O₂ (Figure SD6), sequential stopped-flow double-mixing reaction between preformed Compound II and 2.5–25 equiv of TCP at pH 8 (Figure SD7), EPR spectrum of the radical formed from the reaction between ferric DHP B containing 1 equiv of TCP and a 10-fold excess of H₂O₂ (Figure SD8), titration of ferric DHP B with sodium dithionite (Figure SD9), UV–visible spectroscopic monitoring of the reaction between ferrous DHP B and H₂O₂

yielding Compound II in the absence (Figure SD10) and presence (Figures SD11 and SD12) of TCP, UV–visible spectroscopic monitoring of the reaction of oxyferrous DHP B containing TCP with H₂O₂ yielding Compound II (Figures SD13–SD15), and ³¹P NMR spectra of DIPPMO in the presence of H₂O₂, TCP, and ferric DHP B, oxyferrous DHP B, and HRP (Figure SD16). This material is available free of charge via the Internet at <http://pubs.acs.org>.

AUTHOR INFORMATION

Corresponding Author

*Department of Chemistry, North Carolina State University, Raleigh, NC 27695. Phone: (919) 513-0680. Fax: (919) 515-8920. E-mail: Reza_Ghiladi@ncsu.edu.

Funding Sources

This project was supported by the North Carolina State University Molecular Biotechnology Training Program through a National Institutes of Health T32 Biotechnology Traineeship grant (J.D.) and Army Research Office Grant 57861-LS (R.A.G.).

ABBREVIATIONS

DHP, dehaloperoxidase; Hb, hemoglobin; Mb, myoglobin; HhMb, horse heart myoglobin; DCP, 2,4-dichlorophenol; TBP, 2,4,6-tribromophenol; TCP, 2,4,6-trichlorophenol; TFP, 2,4,6-trifluorophenol; TXP, trihalophenol; DXQ, dihalophenol; RFQ-CW-EPR, rapid-freeze-quench continuous wave electron paramagnetic resonance; Compound I, two-electron-oxidized heme center when compared to the ferric form, commonly known as an Fe^{IV}=O porphyrin π -cation radical; Compound II, one-electron-oxidized heme center when compared to the ferric form, commonly known as an Fe^{IV}=O or Fe^{IV}-OH species; Compound III, oxyferrous [Fe^{II}-O₂ or Fe^{III}-(O₂⁻)] state of the enzyme; Compound ES, two-electron-oxidized state containing both a ferryl center (Fe^{IV}=O) and an amino acid (tryptophanyl or tyrosyl) radical, analogous to Compound ES in cytochrome *c* peroxidase; Compound RH, “reversible heme” state of dehaloperoxidase, formed from the decay of Compound ES in the absence of cosubstrate; 5cHS, five-coordinate high-spin heme; 6cHS, six-coordinate high-spin heme; 6cLS, six-coordinate low-spin heme.

REFERENCES

- (1) Woodin, S. A. (1991) Recruitment of Infauna: Positive or Negative Cues. *Am. Zool.* 31, 797–807.
- (2) Woodin, S. A., Walla, M. D., and Lincoln, D. E. (1987) Occurrence of Brominated Compounds in Soft-Bottom Benthic Organisms. *J. Exp. Mar. Biol. Ecol.* 107, 209–217.
- (3) Chen, Y. P., Lincoln, D. E., Woodin, S. A., and Lovell, C. R. (1991) Purification and Properties of a Unique Flavin-Containing Chloroperoxidase from the Capitellid Polychaete *Notomastus lobatus*. *J. Biol. Chem.* 266, 23909–23915.
- (4) Roach, M. P., Chen, Y. P., Woodin, S. A., Lincoln, D. E., Lovell, C. R., and Dawson, J. H. (1997) *Notomastus lobatus* chloroperoxidase and *Amphitrite ornata* dehaloperoxidase both contain histidine as their proximal heme iron ligand. *Biochemistry* 36, 2197–2202.
- (5) Lincoln, D. E., Fielman, K. T., Marinelli, R. L., and Woodin, S. A. (2005) Bromophenol accumulation and sediment contamination by the marine annelids *Notomastus lobatus* and *Thelepus crispus*. *Biochem. Syst. Ecol.* 33, 559–570.
- (6) King, G. M. (1986) Inhibition of Microbial Activity in Marine Sediments by a Bromophenol from a Hemichordate. *Nature* 323, 257–259.

- (7) Fielman, K. T., and Targett, N. M. (1995) Variation of 2,3,4-Tribromopyrrole and Its Sodium Sulfamate Salt in the Hemichordate *Saccoglossus kowalevskii*. *Mar. Ecol. Prog. Ser.* 116, 125–136.
- (8) Chen, Y. P., Woodin, S. A., Lincoln, D. E., and Lovell, C. R. (1996) An unusual dehalogenating peroxidase from the marine terebellid polychaete *Amphitrite ornata*. *J. Biol. Chem.* 271, 4609–4612.
- (9) Osborne, R. L., Taylor, L. O., Han, K. P., Ely, B., and Dawson, J. H. (2004) *Amphitrite ornata* dehaloperoxidase: Enhanced activity for the catalytically active globin using MCPBA. *Biochem. Biophys. Res. Commun.* 324, 1194–1198.
- (10) Feducia, J., Dumariéh, R., Gilvey, L. B., Smirnova, T., Franzen, S., and Ghiladi, R. A. (2009) Characterization of dehaloperoxidase compound ES and its reactivity with trihalophenols. *Biochemistry* 48, 995–1005.
- (11) Chen, Z., de Serrano, V., Betts, L., and Franzen, S. (2009) Distal histidine conformational flexibility in dehaloperoxidase from *Amphitrite ornata*. *Acta Crystallogr. D* 65, 34–40.
- (12) Davis, M. F., Gracz, H., Vendeix, F. A., de Serrano, V., Somasundaram, A., Decatur, S. M., and Franzen, S. (2009) Different modes of binding of mono-, di-, and trihalogenated phenols to the hemoglobin dehaloperoxidase from *Amphitrite ornata*. *Biochemistry* 48, 2164–2172.
- (13) Smirnova, T. I., Weber, R. T., Davis, M. F., and Franzen, S. (2008) Substrate binding triggers a switch in the iron coordination in dehaloperoxidase from *Amphitrite ornata*: HYSORE experiments. *J. Am. Chem. Soc.* 130, 2128–2129.
- (14) Miksovská, J., Horsa, S., Davis, M. F., and Franzen, S. (2008) Conformational dynamics associated with photodissociation of CO from dehaloperoxidase studied using photoacoustic calorimetry. *Biochemistry* 47, 11510–11517.
- (15) Nienhaus, K., Nickel, E., Davis, M. F., Franzen, S., and Nienhaus, G. U. (2008) Determinants of substrate internalization in the distal pocket of dehaloperoxidase hemoglobin of *Amphitrite ornata*. *Biochemistry* 47, 12985–12994.
- (16) Franzen, S., Gilvey, L. B., and Belyea, J. L. (2007) The pH dependence of the activity of dehaloperoxidase from *Amphitrite ornata*. *Biochim. Biophys. Acta* 1774, 121–130.
- (17) de Serrano, V., Chen, Z., Davis, M. F., and Franzen, S. (2007) X-ray crystal structural analysis of the binding site in the ferric and oxiferrous forms of the recombinant heme dehaloperoxidase cloned from *Amphitrite ornata*. *Acta Crystallogr. D* 63, 1094–1101.
- (18) Franzen, S., Jasaitis, A., Belyea, J., Brewer, S. H., Casey, R., MacFarlane, A. W. t., Stanley, R. J., Vos, M. H., and Martin, J. L. (2006) Hydrophobic distal pocket affects NO-heme geminate recombination dynamics in dehaloperoxidase and H64V myoglobin. *J. Phys. Chem. B* 110, 14483–14493.
- (19) Franzen, S., Belyea, J., Gilvey, L. B., Davis, M. F., Chaudhary, C. E., Sit, T. L., and Lommel, S. A. (2006) Proximal cavity, distal histidine, and substrate hydrogen-bonding mutations modulate the activity of *Amphitrite ornata* dehaloperoxidase. *Biochemistry* 45, 9085–9094.
- (20) Belyea, J., Belyea, C. M., Lappi, S., and Franzen, S. (2006) Resonance Raman study of ferric heme adducts of dehaloperoxidase from *Amphitrite ornata*. *Biochemistry* 45, 14275–14284.
- (21) Osborne, R. L., Coggins, M. K., Raner, G. M., Walla, M., and Dawson, J. H. (2009) The mechanism of oxidative halophenol dehalogenation by *Amphitrite ornata* dehaloperoxidase is initiated by H₂O₂ binding and involves two consecutive one-electron steps: Role of ferryl intermediates. *Biochemistry* 48, 4231–4238.
- (22) Osborne, R. L., Coggins, M. K., Walla, M., and Dawson, J. H. (2007) Horse heart myoglobin catalyzes the H₂O₂-dependent oxidative dehalogenation of chlorophenols to DNA-binding radicals and quinones. *Biochemistry* 46, 9823–9829.
- (23) Osborne, R. L., Raner, G. M., Hager, L. P., and Dawson, J. H. (2006) *C. fumago* chloroperoxidase is also a dehaloperoxidase: Oxidative dehalogenation of halophenols. *J. Am. Chem. Soc.* 128, 1036–1037.
- (24) Osborne, R. L., Sumithran, S., Coggins, M. K., Chen, Y. P., Lincoln, D. E., and Dawson, J. H. (2006) Spectroscopic characterization of the ferric states of *Amphitrite ornata* dehaloperoxidase and *Notomastus lobatus* chloroperoxidase: His-ligated peroxidases with globin-like proximal and distal properties. *J. Inorg. Biochem.* 100, 1100–1108.
- (25) Han, K., Woodin, S. A., Lincoln, D. E., Fielman, K. T., and Ely, B. (2001) *Amphitrite ornata*, a marine worm, contains two dehaloperoxidase genes. *Mar. Biotechnol.* 3, 287–292.
- (26) D'Antonio, J., D'Antonio, E. L., Thompson, M. K., Bowden, E. F., Franzen, S., Smirnova, T., and Ghiladi, R. A. (2010) Spectroscopic and mechanistic investigations of dehaloperoxidase B from *Amphitrite ornata*. *Biochemistry* 49, 6600–6616.
- (27) Dunford, H. B., and Stillman, J. S. (1976) Function and Mechanism of Action of Peroxidases. *Coord. Chem. Rev.* 19, 187–251.
- (28) Du, J., Sono, M., and Dawson, J. H. (2010) Functional Switching of *Amphitrite ornata* Dehaloperoxidase from O₂-Binding Globin to Peroxidase Enzyme Facilitated by Halophenol Substrate and H₂O₂. *Biochemistry* 49, 6064–6069.
- (29) Matsui, T., Ozaki, S., Liong, E., Phillips, G. N., Jr., and Watanabe, Y. (1999) Effects of the location of distal histidine in the reaction of myoglobin with hydrogen peroxide. *J. Biol. Chem.* 274, 2838–2844.
- (30) Finzel, B. C., Poulos, T. L., and Kraut, J. (1984) Crystal structure of yeast cytochrome c peroxidase refined at 1.7-Å resolution. *J. Biol. Chem.* 259, 13027–13036.
- (31) Phillips, G. N., Jr., Arduini, R. M., Springer, B. A., and Sligar, S. G. (1990) Crystal structure of myoglobin from a synthetic gene. *Proteins* 7, 358–365.
- (32) Gajhede, M., Schuller, D. J., Henriksen, A., Smith, A. T., and Poulos, T. L. (1997) Crystal structure of horseradish peroxidase C at 2.15 Å resolution. *Nat. Struct. Biol.* 4, 1032–1038.
- (33) de Serrano, V., D'Antonio, J., Franzen, S., and Ghiladi, R. A. (2010) Structure of dehaloperoxidase B at 1.58 Å resolution and structural characterization of the AB dimer from *Amphitrite ornata*. *Acta Crystallogr. D* 66, 529–538.
- (34) LaCount, M. W., Zhang, E., Chen, Y. P., Han, K., Whitton, M. M., Lincoln, D. E., Woodin, S. A., and Lebioda, L. (2000) The crystal structure and amino acid sequence of dehaloperoxidase from *Amphitrite ornata* indicate common ancestry with globins. *J. Biol. Chem.* 275, 18712–18716.
- (35) Lebioda, L., LaCount, M. W., Zhang, E., Chen, Y. P., Han, K., Whitton, M. M., Lincoln, D. E., and Woodin, S. A. (1999) An enzymatic globin from a marine worm. *Nature* 401, 445.
- (36) Beers, R. F., Jr., and Sizer, I. W. (1952) A spectrophotometric method for measuring the breakdown of hydrogen peroxide by catalase. *J. Biol. Chem.* 195, 133–140.
- (37) Zoia, L., and Argyropoulos, D. S. (2009) Phenoxy radical detection using P-31 NMR spin trapping. *J. Phys. Org. Chem.* 22, 1070–1077.
- (38) Mayhew, S. G. (1978) The redox potential of dithionite and SO₂ from equilibrium reactions with flavodoxins, methyl viologen and hydrogen plus hydrogenase. *Eur. J. Biochem.* 85, 535–547.
- (39) Kizek, R., Vacek, J., Trnkova, L., and Jelen, F. (2004) Cyclic voltammetric study of the redox system of glutathione using the disulfide bond reductant tris(2-carboxyethyl)phosphine. *Bioelectrochemistry* 63, 19–24.
- (40) Heineman, W. R., Meckstroth, M. L., Norris, B. J., and Su, C.-H. (1979) Optically transparent thin layer electrode techniques for the study of biological redox systems. *J. Electroanal. Chem.* 104, 577–585.
- (41) Ball, E. G. (1937) Studies on Oxidation-Reduction XXIII: Ascorbic Acid. *J. Biol. Chem.* 118, 219–239.
- (42) Belyea, J., Gilvey, L. B., Davis, M. F., Godek, M., Sit, T. L., Lommel, S. A., and Franzen, S. (2005) Enzyme function of the globin dehaloperoxidase from *Amphitrite ornata* is activated by substrate binding. *Biochemistry* 44, 15637–15644.
- (43) Lardinois, O. M., and Ortiz de Montellano, P. R. (2004) Autoreduction of ferryl myoglobin: Discrimination among the three tyrosine and two tryptophan residues as electron donors. *Biochemistry* 43, 4601–4610.
- (44) Giulivi, C., and Cadenas, E. (1994) Ferrylmyoglobin: Formation and chemical reactivity toward electron-donating compounds. *Methods Enzymol.* 233, 189–202.

- (45) Herold, S., and Rehmann, F. J. (2003) Kinetics of the reactions of nitrogen monoxide and nitrite with ferryl hemoglobin. *Free Radical Biol. Med.* 34, 531–545.
- (46) Giulivi, C., and Davies, K. J. (1994) Hydrogen peroxide-mediated ferrylhemoglobin generation in vitro and in red blood cells. *Methods Enzymol.* 231, 490–496.
- (47) Yadav, R. K., Dolai, S., Pal, S., and Adak, S. (2008) Role of tryptophan-208 residue in cytochrome c oxidation by ascorbate peroxidase from *Leishmania major*: Kinetic studies on Trp208Phe mutant and wild type enzyme. *Biochim. Biophys. Acta* 1784, 863–871.
- (48) Marquez, L. A., Quitariano, M., Zilinskas, B. A., and Dunford, H. B. (1996) Kinetic and spectral properties of pea cytosolic ascorbate peroxidase. *FEBS Lett.* 389, 153–156.
- (49) Hewson, W. D., and Hager, L. P. (1979) Oxidation of horseradish peroxidase compound II to compound I. *J. Biol. Chem.* 254, 3182–3186.
- (50) Belevich, I., Borisov, V. B., and Verkhovsky, M. I. (2007) Discovery of the true peroxy intermediate in the catalytic cycle of terminal oxidases by real-time measurement. *J. Biol. Chem.* 282, 28514–28519.
- (51) Shintaku, M., Matsuura, K., Yoshioka, S., Takahashi, S., Ishimori, K., and Morishima, I. (2005) Absence of a detectable intermediate in the compound I formation of horseradish peroxidase at ambient temperature. *J. Biol. Chem.* 280, 40934–40938.
- (52) Baek, H. K., and Van Wart, H. E. (1989) Elementary steps in the formation of horseradish peroxidase compound I: Direct observation of compound O, a new intermediate with a hyperporphyrin spectrum. *Biochemistry* 28, 5714–5719.
- (53) Egawa, T., Yoshioka, S., Takahashi, S., Hori, H., Nagano, S., Shimada, H., Ishimori, K., Morishima, I., Suematsu, M., and Ishimura, Y. (2003) Kinetic and spectroscopic characterization of a hydroperoxy compound in the reaction of native myoglobin with hydrogen peroxide. *J. Biol. Chem.* 278, 41597–41606.
- (54) Thompson, M. K., Franzen, S., Ghiladi, R. A., Reeder, B. J., and Svistunenko, D. A. (2010) Compound ES of Dehaloperoxidase Decays via Two Alternative Pathways Depending on the Conformation of the Distal Histidine. *J. Am. Chem. Soc.* 132, 17501–17510.
- (55) Lente, G., and Espenson, J. H. (2004) Photoreduction of 2,6-dichloroquinone in aqueous solution: Use of a diode array spectrophotometer concurrently to drive and detect a photochemical reaction. *J. Photochem. Photobiol., A* 163, 249–258.
- (56) Lente, G., and Espenson, J. H. (2004) A kinetic study of the early steps in the oxidation of chlorophenols by hydrogen peroxide catalyzed by a water-soluble iron(III) porphyrin. *New J. Chem.* 28, 847–852.
- (57) Dunford, H. B. (1999) *Heme Peroxidases*, Wiley-VCH, New York.
- (58) Noble, R. W., and Gibson, Q. H. (1970) The reaction of ferrous horseradish peroxidase with hydrogen peroxide. *J. Biol. Chem.* 245, 2409–2413.
- (59) Aviram, I., Wittenberg, A., and Wittenberg, J. B. (1978) The reaction of ferrous leghemoglobin with hydrogen peroxide to form leghemoglobin(IV). *J. Biol. Chem.* 253, 5685–5689.
- (60) Kohler, H., Taurog, A., and Dunford, H. B. (1988) Spectral studies with lactoperoxidase and thyroid peroxidase: Interconversions between native enzyme, compound II, and compound III. *Arch. Biochem. Biophys.* 264, 438–449.
- (61) Jantschko, W., Furtmuller, P. G., Zederbauer, M., Neuschwandtner, K., Jakopitsch, C., and Obinger, C. (2005) Reaction of ferrous lactoperoxidase with hydrogen peroxide and dioxygen: An anaerobic stopped-flow study. *Arch. Biochem. Biophys.* 434, 51–59.
- (62) Jantschko, W., Georg Furtmuller, P., Zederbauer, M., Lanz, M., Jakopitsch, C., and Obinger, C. (2003) Direct conversion of ferrous myeloperoxidase to compound II by hydrogen peroxide: An anaerobic stopped-flow study. *Biochem. Biophys. Res. Commun.* 312, 292–298.
- (63) Jakopitsch, C., Wanasinghe, A., Jantschko, W., Furtmuller, P. G., and Obinger, C. (2005) Kinetics of interconversion of ferrous enzyme, compound II and compound III of wild-type *Synechocystis* catalase-peroxidase and Y249F. Proposal for the catalytic mechanism. *J. Biol. Chem.* 280, 9037–9042.
- (64) Tanaka, M., Matsuura, K., Yoshioka, S., Takahashi, S., Ishimori, K., Hori, H., and Morishima, I. (2003) Activation of hydrogen peroxide in horseradish peroxidase occurs within approximately 200 micro s observed by a new freeze-quench device. *Biophys. J.* 84, 1998–2004.
- (65) Ichikawa, Y., Nakajima, H., and Watanabe, Y. (2006) Characterization of peroxide-bound heme species generated in the reaction of thermally tolerant cytochrome c552 with hydrogen peroxide. *ChemBioChem* 7, 1582–1589.
- (66) Denisov, I. G., Dawson, J. H., Hager, L. P., and Sligar, S. G. (2007) The ferric-hydroperoxy complex of chloroperoxidase. *Biochem. Biophys. Res. Commun.* 363, 954–958.
- (67) Denisov, I. G., Makris, T. M., and Sligar, S. G. (2002) Formation and decay of hydroperoxy-ferric heme complex in horseradish peroxidase studied by cryoradiolysis. *J. Biol. Chem.* 277, 42706–42710.
- (68) Brittain, T., Baker, A. R., Butler, C. S., Little, R. H., Lowe, D. J., Greenwood, C., and Watmough, N. J. (1997) Reaction of variant sperm-whale myoglobins with hydrogen peroxide: The effects of mutating a histidine residue in the haem distal pocket. *Biochem. J.* 326 (Part 1), 109–115.
- (69) Ozaki, S., Inada, Y., and Watanabe, Y. (1998) Characterization of polyethylene glycolated horseradish peroxidase in organic solvents: Generation and stabilization of transient catalytic intermediates at low temperature. *J. Am. Chem. Soc.* 120, 8020–8025.
- (70) Franzen, S., Roach, M. P., Chen, Y. P., Dyer, R. B., Woodruff, W. H., and Dawson, J. H. (1998) The unusual reactivities of *Amphirite ornata* dehaloperoxidase and *Notomastus lobatus* chloroperoxidase do not arise from a histidine imidazolate proximal heme iron ligand. *J. Am. Chem. Soc.* 120, 4658–4661.
- (71) Alayash, A. I., Ryan, B. A., Eich, R. F., Olson, J. S., and Cashion, R. E. (1999) Reactions of sperm whale myoglobin with hydrogen peroxide. Effects of distal pocket mutations on the formation and stability of the ferryl intermediate. *J. Biol. Chem.* 274, 2029–2037.
- (72) Shimahara, H., Yoshida, T., Shibata, Y., Shimizu, M., Kyogoku, Y., Sakiyama, F., Nakazawa, T., Tate, S., Ohki, S. Y., Kato, T., Moriyama, H., Kishida, K., Tano, Y., Ohkubo, T., and Kobayashi, Y. (2007) Tautomerism of histidine 64 associated with proton transfer in catalysis of carbonic anhydrase. *J. Biol. Chem.* 282, 9646–9656.
- (73) Jewsbury, P., and Kitagawa, T. (1994) The distal residue-CO interaction in carbonmonoxy myoglobins: A molecular dynamics study of two distal histidine tautomers. *Biophys. J.* 67, 2236–2250.
- (74) Rovira, C., Schulze, B., Eichinger, M., Evanseck, J. D., and Parrinello, M. (2001) Influence of the heme pocket conformation on the structure and vibrations of the Fe-CO bond in myoglobin: A QM/MM density functional study. *Biophys. J.* 81, 435–445.
- (75) De Angelis, F., Jarzecki, A. A., Car, R., and Spiro, T. G. (2005) Quantum chemical evaluation of protein control over heme ligation: CO/O₂ discrimination in myoglobin. *J. Phys. Chem. B* 109, 3065–3070.
- (76) Lukin, J. A., Simplaceanu, V., Zou, M., Ho, N. T., and Ho, C. (2000) NMR reveals hydrogen bonds between oxygen and distal histidines in oxyhemoglobin. *Proc. Natl. Acad. Sci. U.S.A.* 97, 10354–10358.
- (77) Phillips, G. N., Teodoro, M. L., Li, T. S., Smith, B., and Olson, J. S. (1999) Bound CO is a molecular probe of electrostatic potential in the distal pocket of myoglobin. *J. Phys. Chem. B* 103, 8817–8829.
- (78) Rovira, C. (2003) Role of the His64 residue on the properties of the Fe-CO and Fe-O-2 bonds in myoglobin. A CHARMM/DFT study. *THEOCHEM* 632, 309–321.
- (79) Rovira, C. (2003) The structure and dynamics of the Fe-CO bond in myoglobin. *J. Phys.: Condens. Matter* 15, S1809–S1822.